



Interaction of nanostructured TiO₂ biointerfaces with stem cells and biofilm-forming bacteria



Mukta Kulkarni^a, Ita Junkar^{b,*}, Petr Humpolíček^{c,d,*}, Zdenka Capáková^c, Katarzyna Anna Radaszkiewicz^e, Nikola Mikušová^{c,d}, Jiří Pacherník^e, Marián Lehocký^c, Aleš Iglíč^b, Markéta Hanáčková^e, Miran Mozetič^b

^a Laboratory of Biophysics, Faculty of Electrical Engineering, University of Ljubljana, Ljubljana SI-1000, Slovenia

^b Jožef Stefan Institute, Jamova 39, Ljubljana 1000, Slovenia

^c Centre of Polymer Systems, Tomas Bata University in Zlin, T.G.M. Sq. 5555, 760 01 Zlin, Czech Republic

^d Polymer Centre, Faculty of Technology, Tomas Bata University in Zlin, 762 72 Zlin, Czech Republic

^e Department of Experimental Biology, Faculty of Science, Masaryk University, 625 00 Brno, Czech Republic

ARTICLE INFO

Article history:

Received 27 October 2016

Received in revised form 15 March 2017

Accepted 17 March 2017

Available online 22 March 2017

Keywords:

Nanotubes

Titanium

Biofilm

Stem cells

Surface morphology

ABSTRACT

Nanostructured TiO₂ nanotubes (NTs) of diameters from 15 to 100 nm were fabricated by an electrochemical anodization process. Biofilm-positive strains of *Bacillus cereus* and *Pseudomonas aeruginosa* behaved similarly on all TiO₂ NTs as well as on native titanium (Ti) foil. The adhesion and growth of mesenchymal stem cells (MSc), embryonic stem cells (ESc), and pure cardiomyocytes derived from ESc exhibited significant differences. MSc as well as ESc were, in contrast to cardiomyocytes, able to adhere, and grow on TiO₂ NTs. A correlation between NTs diameter and cell behaviour was however observed in the case of MSc and ESc. MSc were not in a physiological state in the case of 100 nm TiO₂ NTs, while ESc were not able to grow on 15 nm TiO₂ NTs. It can be stated that these differences can be assigned to different diameters of the NTs but not to the chemistry of the surface. This is the first study describing the comprehensive behaviour of both eukaryotic and prokaryotic cells on TiO₂ NTs. On the basis of obtained results, it can be concluded that new generation of medical devices providing selective cell behaviour can be fabricated by optimizing the nanoscale morphology of TiO₂.

© 2017 Elsevier B.V. All rights reserved.

1. Introduction

Titanium and its alloys are commonly employed in medical implants, but progress in nanotechnologies together with new findings indicating the importance of nanoscale morphology on cell behaviour; which open the door to new applications utilizing nanostructured titanium surfaces. This emerges from the fact that the interaction between cells or tissues and any foreign material depends not only on the chemical composition of the material, but also on its nanoscale morphology. Because of this, the interaction of cells with nanostructured surfaces is the subject of intensive research. To improve the biological, chemical, and mechanical properties of biomaterials, significant research efforts have been made to fabricate suitable morphologies which could offer the desired biological response (reviewed by Kulkarni et al. [9]). In recent years, several methods have been developed to produce nanoscale morphologies on titanium (Ti) surfaces. One of these methods, the electrochemical anodization of Ti, is a powerful tool for controlling the

nanoscale morphology of Ti. For example, titanium dioxide (TiO₂) NTs with well-controlled morphology can be synthesized by the electrochemical anodization of Ti using a two-electrode system. Previously, self-organized TiO₂ NTs layers fabricated in fluoride containing electrolytes which were studied intensively [1,12]. Later it was shown that water content in the electrolyte is the critical factor that determines whether self-ordered oxide NTs or nanopores are formed during electrochemical anodization; it is thought that tube formation originates from ordered porous oxide by a “pore-wall-splitting” mechanism [20]. By tailoring the anodization parameters (applied voltage, anodization time, and concentrations of chemicals), TiO₂ NTs of different diameters ranging from 15 nm to 150 nm and different lengths can be obtained.

Knowledge about the interaction of various nanostructured TiO₂ surfaces with cells is one of the crucial factors influencing the use of TiO₂ in medical applications (e.g. orthopaedic, vascular, dental implants). Recently, studies focusing on the interaction between TiO₂ NTs and various cell types have emerged. Among the most commonly studied cell types in this context are mesenchymal stem cells (MSc). For example, in the work of Bauer et al. [3], MSc exhibited the best adhesion on NTs of 15 nm in diameter, the adhesion decreasing as the NTs diameter gets increased further. This inverse proportionality was also confirmed in other works on MSc adhesion and proliferation [5,

* Corresponding authors: P. Humpolíček, Polymer Centre, Faculty of Technology, Tomas Bata University in Zlin, T.G.M. Sq. 5555, 760 01 Zlin, Czech Republic and I. Junkar, Jožef Stefan Institute, Jamova cesta 39, Ljubljana SI-1000, Slovenia.

E-mail addresses: ita.junkar@ijs.si (I. Junkar), humpolicek@ft.utb.cz (P. Humpolíček).

17,21]. In contrast, results using different cell lines appeared to be different. A study by Yu et al. indicated that the proliferation of pre-osteoblasts was similar for all used diameters of NTs (20–120 nm) [22]. However, the performance of human coronary artery endothelial cells (HCAEC) was shown to decrease with increasing NTs diameter, as HCAEC function was far less optimal on Ti NTs of 100 nm in diameter [4]. To the best of our knowledge, there are no studies dealing with the influence of TiO₂ NTs on embryonic stem cells or cardiomyocytes, despite the fact that these cell types are of great interest; ESC are at the centre of attention due to their naive phenotype, while cardiomyocytes are of particular importance because of their interaction with Ti materials used in cardiac support devices.

Biofilm formation, which is highly relevant for all implantable materials, is another parameter worthy of study. It is a well-known fact that a significant number of revision surgeries are required due to biomaterial infections, which increase medical costs and can even, be life threatening for patients. Due to the rise of antibiotic-resistant bacterial strains, it is also of primary importance to inhibit the growth of biofilms on implantable materials by influencing their surface properties. Various studies have already reported that nanotubular features could reduce bacterial adhesion [15]. For example, Puckett et al. reported that lower amounts of live *Staphylococcus aureus*, *Staphylococcus epidermidis*, and *Pseudomonas aeruginosa* were found on nanorough Ti compared to conventional (non-nanorough) Ti [18]. The nanorough surface was produced by electron beam evaporation. In the same study, adhesion of the above mentioned bacteria on electrochemically anodized titanium NTs of 60–70 nm in diameter was also studied. Interestingly, no reduction in bacterial adhesion was observed on these surfaces. In another study by Anitha et al., the adhesion of *Shewanella oneidensis* MR-1 cells on TiO₂ NTs with different pore diameters (20–140 nm) was studied [2]. It was observed that biofilm formation increased with decreasing NT diameter; thus, the greatest degree of bacterial cell adhesion (biofilm formation) was observed for 20 nm NTs. This indicates that by appropriately structuring the surface of titanium, it may be possible to stimulate the desired biological response.

2. Experimental section

2.1. Fabrication of TiO₂ nanotubes

TiO₂ NTs were fabricated by the electrochemical anodization of Ti foil (Advent Research Materials, England) of 0.1 mm thickness (99.6% purity), as published previously [9,10]. Briefly, NTs were obtained by a two-step anodization method, where, in the first step, a pre-patterned surface was obtained by electrochemical anodization of Ti foil in an ethylene glycol (EG) electrolyte (with 1 M H₂O and 0.1 M NH₄F) at 35 V for 2 h, followed by ultrasonication in deionized water (DI) water in order to remove the grown nanotubular layer. In the second step, electrochemical anodization was conducted using EG electrolyte containing 8 M water and 0.2 M hydrofluoric acid (40% HF solution). The anodization conditions are presented in Table 1. All reagents were purchased from Sigma–Aldrich, Germany and used without further purification.

2.2. Scanning electron microscopy (SEM)

High contrast images of TiO₂ NTs were obtained by scanning electron microscopy (Hitachi FE-SEM S4800). All samples were used

without gold sputtering as the NTs samples already display images with reasonably good contrast.

2.3. Atomic force microscopy (AFM)

Topographic features of TiO₂ NTs were examined by means of Atomic Force Microscopy (Solver PRO, TiO₂ NTs -MDT, Russia) in tapping mode in air. The TiO₂ NTs were analysed using the standard Si cantilever with a force constant of 22 N/m, and at a resonance frequency of 325 kHz. The average surface roughness (Ra) across a 3 × 3 μm² area was measured from representative images. The results are shown as the average Ra from five different areas.

2.4. Water contact angle measurements

Surface wettability was measured 25 h after TiO₂ NTs were produced by anodization and stored in sealed plastic containers at room temperature in order to prevent surface ageing effects (changes in hydrophilic character). All NT surfaces were analysed after one week of fabrication. Droplet of 3 μL DI water was placed on the surface of NTs and the contact angle was determined from high resolution images. For each sample, six measurements were performed in order to obtain statistically robust data.

2.5. X-ray photoelectron spectroscopy (XPS)

The samples were analysed by means of X-ray photoelectron spectroscopy (XPS or ESCA) using a PHI-TFA XPS spectrometer (Physical Electronics Inc.). Samples were placed on a sample holder and introduced into an ultra-high vacuum spectrometer. The analysed area was 0.4 mm in diameter and the analysed depth was about 3–5 nm; this high surface sensitivity is a general characteristic of the XPS method. X-ray radiation from a monochromatic Al source with a photon energy of 1486.6 eV was used to excite the surface, and high-energy resolution spectra were acquired by an energy analyser operating at a resolution of approximately 0.6 eV and a pass energy of 29 eV. During data processing, spectra were aligned by setting the C 1s peak at 285.0 eV, characteristic for C–C bonds. The accuracy of binding energies was approximately ±0.3 eV. The quantification of surface composition was determined from XPS peak intensities taking into account relative sensitivity factors provided by the instrument manufacturer. Three different XPS measurements were performed for each sample and the average composition was calculated.

The survey and high resolution spectra of C 1s, O 1s and Ti 2p were recorded for Ti foil and TiO₂ NTs of different diameters one week after fabrication.

2.6. Biointerface properties

The biointerface properties of Ti foil and TiO₂ NT surfaces were therefore determined by both biofilm positive strains of bacteria (prokaryotic cells) and mesenchymal stem cells (MSC), embryonic stem cells (ESC), and pure cardiomyocytes derived from embryonic stem cells (eukaryotic cells). A sample of 1 cm² size was used for all tests. All tests were performed in quadruplicates and repeated for three times. Prior to testing, the samples were sterilized using UV light for 30 min.

2.6.1. Bacterial biofilm formation

To detect biofilm formation on pristine Ti foil and TiO₂ NTs, two biofilm-forming bacterial strains were used, *Bacillus cereus* (Czech Collection of Microorganisms 2010) and *Pseudomonas aeruginosa* (Czech Collection of Microorganisms 3955). To inoculate the bacteria, 2 mL of Tryptone soya Broth (Himedia, India) was added to each sample in the Petri dish and subsequently seeded by 20 μL of the bacterial suspensions (2. degree of McFarland standard in physiological solution). After

Table 1
Anodization conditions for different TiO₂ NTs.

TiO ₂ NTs diameter	Electrolyte	Potential	Anodization time
15 nm	EG + 8 M water + 0.2 M HF	10 V	2.5 h
50 nm	EG + 8 M water + 0.2 M HF	20 V	2.5 h
100 nm	EG + 8 M water + 0.2 M HF	58 V	2.5 h

inoculation, samples corresponding to *B. cereus* and *P. aeruginosa* were incubated for 48 h at 37 °C and 30 °C, respectively.

After incubation, the contents of Petri dishes were removed and the samples gently rinsed with physiological solution and air-dried. The number of bacterial cells was measured by ATP kit SL (Biothema, Sweden).

2.6.2. Cytocompatibility

The cyto-compatibilities of Ti foil and TiO₂ NTs were tested using three different cell types: mesenchymal stem cells (MSc), the R1 embryonic stem cell (ESc) line [14], and HG8 clone cardiomyocytes derived from these R1 ESc, carrying cardiomyocyte specific myosin heavy chain alpha promoter-dependent selection vector [7], kindly donated by Dr. Field, L.J. (For more information on the cardiomyocytes, see [6, 19]).

MSc were cultivated in ATCC-formulated Dulbecco's Modified Eagle's Medium (BioSera, France) containing 20% of calf serum (BioSera, France), 100 U mL⁻¹ Penicillin/Streptomycin (GE Healthcare HyClone, United Kingdom) and 0.05 mM mercaptoethanol (Serva, Germany). ESc were propagated in an undifferentiated state by culturing on gelatinized tissue culture dishes using complete Dulbecco's Modified Eagle's Medium containing 15% fetal calf serum, 100 U mL⁻¹ Penicillin, 0.1 mg mL⁻¹ Streptomycin, 100 mM non-essential amino acids (all from Gibco-Invitrogen; US), 0.05 mM β-mercaptoethanol (Sigma-Aldrich; US), and 1000 U mL⁻¹ of leukemia inhibitory factor (Chemicon; US). Cardiomyocytes were cultured in Dulbecco's Modified Eagle's Medium - F12 media supplemented by 7.5% fetal calf serum, 100 U mL⁻¹ Penicillin, 0.1 mg mL⁻¹ Streptomycin, 100 mM, 0.025 mM β-mercaptoethanol (Sigma-Aldrich; US), and Insulin, Transferin and Selenium (ITS supplement, Gibco-Invitrogen; US).

The cyto-compatibility test was designed as follows: MSc were seeded onto native surfaces at a concentration of 5 × E4 cells per cm² and cultivated for 48 h. Subsequently DNA staining with Hoechst 33258 (5 μg mL⁻¹ Invitrogen USA) and actin filament staining (ActinRed™ 555, Thermo Fisher Scientific USA) was used to determine cell morphology. ESc and cardiomyocytes were cultivated either on native surfaces or on surfaces coated with gelatine.

ESc R1 cells were seeded at a density of 10 × E4 cells per cm². After 48 h, cells were either uploaded by Calcein AM (10 μM) (Invitrogen; US), which coloured only viable cells, or fixed by 2% formaldehyde and visualized through nuclei staining by DAPI (10 ng mL⁻¹, Sigma). The mass of viable cells was also determined as the level of ATP using Cellular ATP Kit HTS (Biothema, Sweden). Cardiomyocytes were seeded on native surfaces at a density of 10 × E4 cells per cm² and, after 48 h, fixed with 2% formaldehyde and stained by antibody against cardiomyocyte specific myosin heavy chain (MF20 antibody, developed by Drs. Donald and Fischman, was obtained from the Developmental Studies Hybridoma Bank under the auspices of the National Institute of Child Health and Human Development and maintained by the University of Iowa, Department of Biological Sciences). As a secondary antibody, donkey anti-mouse IgG Alexa Fluor 568 antibody was used. Nuclei were counterstained by DAPI (10 ng mL⁻¹, Sigma). Micrographs were taken by means of an inverted Olympus phase contrast microscope (IX 81, Japan).

3. Results and discussion

3.1. Nanoscale morphology and surface chemistry of TiO₂ NTs

The surface properties of both Ti foil and TiO₂ NTs were characterized in terms of surface morphology (using SEM and AFM techniques), wettability, and surface chemistry (using XPS).

The analysis of surface morphology by SEM and AFM techniques revealed that pristine Ti foil had no special morphological features, while a uniform nanotubular structure was observed for electrochemical anodized TiO₂ surfaces (Fig. 1). From SEM images it can easily be observed

that TiO₂ NTs are evenly distributed on the surface and that anodization potentials of 10 V, 20 V and 58 V lead to the formation of TiO₂ NTs of 15, 50 and 100 nm in diameter, respectively (Fig. 1). According to the results of AFM, Ti foil is not completely flat, as the average surface roughness measured on a 3 × 3 μm² area was about 19.3 nm. In the case of NTs, the calculated average surface roughness increased with NTs diameter, from about 11.7 nm for 15 nm NTs, to about 18.6 and 27.9 nm for 50 and 100 nm NTs, respectively. Although penetration of the AFM tip inside the hollow NTs interior is limited, due to the tip radius and the size of the NTs, the calculated roughness values and images obtained provide additional information about the 3D structures of the NTs, these having the specific ability to interact with different cell types. Based on the previously published work we can conclude that the nanotubes have about 1 to 4 μm in height and are stable on the surface [8].

Another important aspect of a biomaterial surface is its wettability [13], which could, together with other surface properties, influence on the biological response. Water contact angle measurements conducted on Ti foil and freshly fabricated TiO₂ NTs indicate that Ti foil is poorly wettable (a water contact angle of about 78°), while TiO₂ NTs are all hydrophilic (a water contact angle of <50). However, it should be noted that fabricated TiO₂ NT surfaces tend to age if exposed to the atmosphere and become hydrophobic, as shown in our previous work [10]. Thus, to ensure the hydrophilic character of the surfaces, all biological experiments were conducted one week after fabrication.

The chemical compositions of Ti foil and TiO₂ NTs of different diameters were determined from XPS survey spectra; the spectra for NT 100 is presented in Fig. 2A. No significant differences in chemical composition were observed between different diameter NTs (Table 2). Moreover, similar surface chemistry was observed for pristine Ti foil. The composition of the top surface layer of Ti foil was approximately 38% carbon, 41% oxygen, 18% titanium, and a few percent nitrogen. In the case of all nanotubular surfaces the chemical composition was very similar; the only difference was in the presence of fluorine on the surface. The fluorine content was about 3–5% and was ascribed to the remains of the electrolyte used for electrochemical anodization. In Fig. 2A, the survey spectra for 100 nm NTs are presented. It can clearly be seen that only C, O, Ti, N and F atoms are present on the surface. Similar survey spectra were also recorded for the other NT diameters as well as for the Ti foil. From the high resolution spectra of C 1s, O 1s, and Ti 2p, which are presented in Figs. 2B–D, no significant differences in peaks among different NT diameters and between NTs and Ti foil were observed. The C 1s peak has a main peak at 284.8 eV, corresponding to C—C and C—H groups, and a small shoulder peak appearing at 288.9 eV, which corresponds to C=O bonds (Fig. 2B). In the case of the O 1s high-resolution scan, a primary peak at a binding energy of about 530.2 eV can be seen, which corresponds to the TiO₂ component (Fig. 2C). In the case of the Ti 2p peak, a doublet peak with maxima at 458.7 eV and 464.5 eV is observed, which is typical for the TiO₂ component (Fig. 2D). Differences in high-resolution peaks among different NTs diameters were not observed, indicating that the binding of C, O and Ti is similar for all NTs.

3.2. Biointerface properties

The interaction of any biomaterial with biological fluids, cells, tissues or the immune system begins on the surface of the material. Therefore, the biointerface properties of any biomaterial or medical device are crucial for its biocompatibility. Titanium and its alloys are commonly employed for medical implants, but progress in nanotechnologies together with new findings indicating the importance of nanoscale morphology on cell behaviour opens the door for the application of titanium nanostructured surfaces.

From a practical point of view, interactions with biofilm-forming species of bacteria are highly relevant, especially in the case of nosocomial infections and implants. Therefore, interactions with *B. cereus* and *P. aeruginosa*, representing both G+ and G– biofilm forming bacteria,

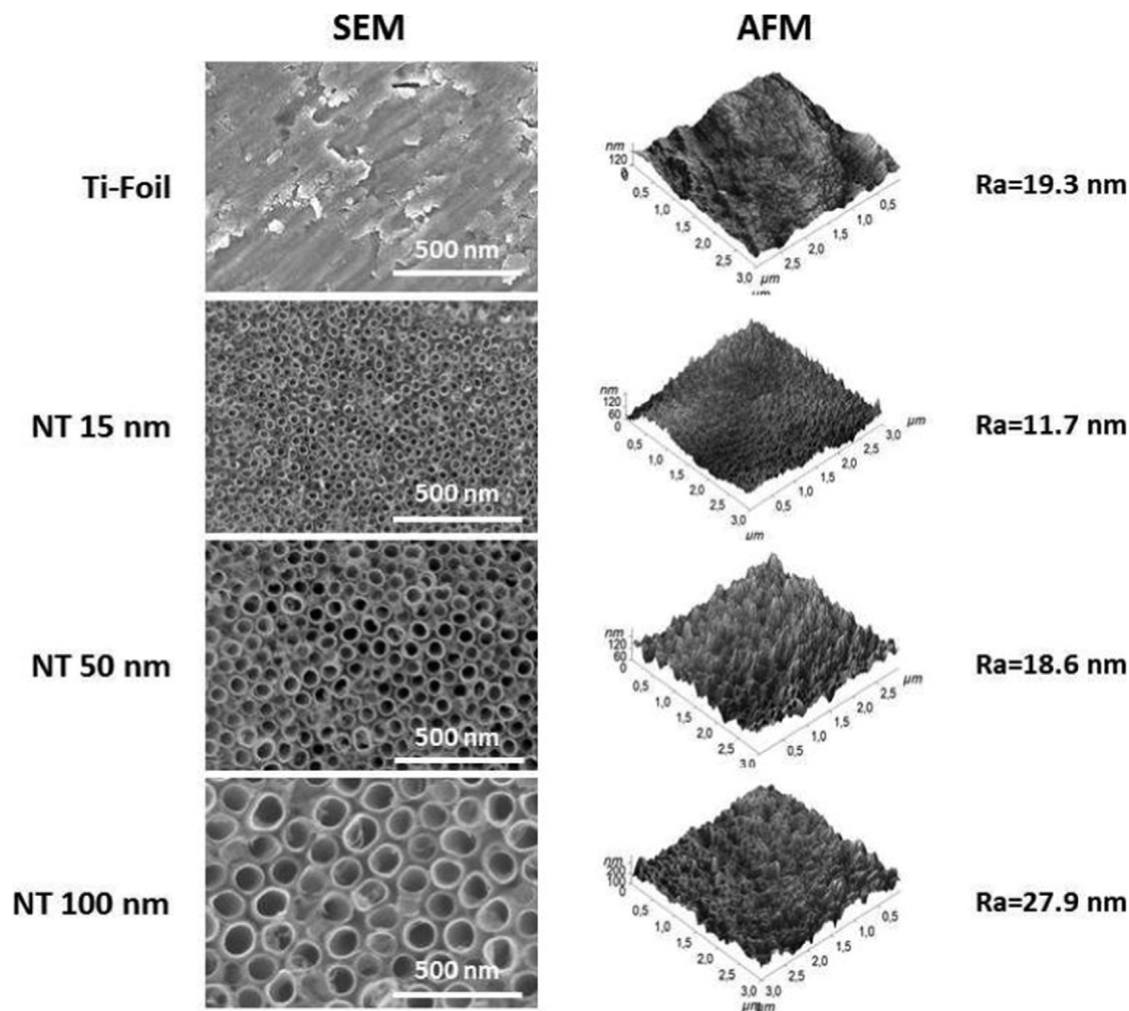


Fig. 1. Surface morphology of Ti foil and TiO_2 NTs determined from images taken by SEM and AFM.

were studied. The results demonstrate that both bacteria can form biofilms with slightly higher amounts on TiO_2 NTs compared to Ti foil (Table 3); however, the differences in our study were not significant. In addition, slightly higher amounts of formed biofilm were observed for *Bacillus cereus* compared to *Pseudomonas aeruginosa*; the differences, however, were also not significant. In this study, biofilm-positive bacterial strains were employed, which differ in many of their properties compared to the planktonic form of bacteria, which were preferentially used in previous works. The findings from this study are therefore comparable to only a few previous studies, mainly the work of Puckett et al., who reported that lower amounts of live *Staphylococcus aureus*, *Staphylococcus epidermidis*, and *Pseudomonas aeruginosa* were found on nanorough Ti compared to conventional (non-nanorough) Ti [18]. In another paper, Anitha et al. studied the adhesion of *Shewanella oneidensis* MR-1 cells on TiO_2 NTs. They found increased biofilm formation with decreasing NT diameter; thus, the highest level of bacterial cell

adhesion (biofilm formation) was observed for 20 nm NTs [2]. The results of the present study are therefore not in accordance with these studies, as we found no significant differences in bacterial behaviour with respect to biofilms formed on Ti.

In the present study, MSC were able to adhere and subsequently grow on all surfaces, although cells behaved differently on TiO_2 NTs of different diameters. On 15 nm TiO_2 NTs (Fig. 3b) and 50 nm TiO_2 NTs (Fig. 3c), the cells exhibited similar morphology and also their quantity was comparable to that found on Ti foil (Fig. 3a). On 100 nm TiO_2 NTs, (Fig. 3d) the cells drastically changed their morphology. The cells did not spread out and their viability was significantly lower (this is evident from the number of dead cells, as only DNA and not the cytoskeleton is seen on the micrograph). The 100 nm TiO_2 NTs can therefore be assigned as having a critical diameter, which initiates different behaviour of mesenchymal stem cells on TiO_2 NTs.

According to Fig. 4, it can be concluded that ESC were able to adhere, grow and survive in spherical compact colonies on both gelatine non-coated and coated surfaces, but with NTs diameter having an important influence. It is important to note that only viable cells were coloured with the dye, so we can also conclude that surface morphology influences the number of viable cells which adhere. ESC seem to be able to behave similarly on Ti foil, TiO_2 NTs 50 nm and TiO_2 NTs 100 nm, but on TiO_2 NTs 15 nm (Fig. 4a) the cells form smaller non-spherical colonies.

To confirm observations from fluorescence microscopy, the quantification of ESC was performed using ATP staining. The first graph (Fig. 5A) shows how the cells behave in contact with native non-gelatine-coated

Table 2

Surface composition of pristine Ti-foil and freshly prepared NTs of 15, 50, and 100 nm in diameter obtained with XPS.

Material	Atomic %					Ratio	
	C	O	Ti	N	F	C/O	Ti/O
Ti-foil	38.3	41.2	18.0	2.5	0.0	0.93	0.44
15 nm	39.2	41.3	15.1	1.3	3.1	0.95	0.36
50 nm	36.2	42.7	16.1	0.8	4.2	0.85	0.38
100 nm	37.6	39.9	16.1	1	5.4	0.94	0.40

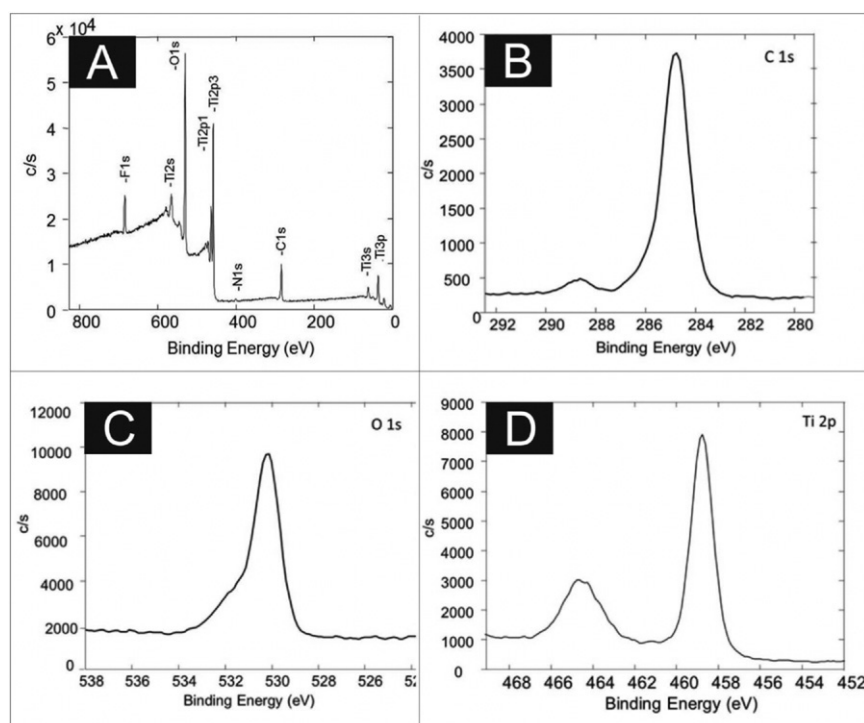


Fig. 2. Surface chemistry determined by XPS analysis; (A) XPS survey spectra for TiO₂ NTs of 100 nm in diameter, and the high resolution scan of TiO₂ NTs of 100 nm in diameter for (B) C 1s, (C) O 1s, and (D) Ti 2p peaks.

surfaces. The results confirm that significantly lower amounts of viable cells was found on the TiO₂ NTs 15 nm sample, compared to both tissue culture plastic and pure Ti foil. 50 nm TiO₂ NTs and 100 nm TiO₂ NTs exhibit comparable abilities with respect to cell adhesion and survival; however, compared to tissue culture plastic their ability is significantly lower. As the gelatinization of surfaces is a frequently used technique for improving surface cyto-compatibility, this technique was also applied on nanostructured titanium surfaces. When the surfaces were coated with gelatine (Fig. 5b), the differences between 15 nm TiO₂ NTs and the other diameter NTs were insignificant. The significant difference found with tissue culture plastic, however, remained. It can be concluded that gelatinization eliminates significant differences between different nanostructures, i.e., differences that were observed previously on freshly fabricated surfaces. Although improvements in ESc cell response on gelatine-covered nanostructured surfaces were observed in the case of 15 nm TiO₂ NTs, the overall influence of gelatinization was not as prominent. Thus, nanotopographic features seem to prevail over the chemical alteration of surfaces covered with gelatine, as the response of ESc to these surfaces was still lower compared to control. The small differences between the results from Calcein staining and ATP are based on the fact that Calcein loading leads to the release of cell colonies from surfaces in a time dependent manner, probably mediated by its toxicity to cells. Based on the results presented in Figs. 4 and 5, it can be concluded that ESc can adhere to and grow on TiO₂ nanostructured surfaces, except on NTs of 15 nm in diameter.

Table 3

Biofilm formation expressed as the number of bacterial cells on an area of 28.3 mm² after 48 h incubation.

Sample	<i>Bacillus cereus</i>	<i>Pseudomonas aeruginosa</i>
Ti foil	1.24×10^6	2.52×10^6
15 nm	66.5×10^6	7.10×10^6
50 nm	16.7×10^6	12.5×10^6
100 nm	52.5×10^6	2.42×10^6

In contrast to MSc and ESc, the ability of cardiomyocytes to adhere to and mainly to survive and grow on all the tested Ti based samples was very limited. From Fig. 6 it is clear that cell artefacts counterstained by DAPI are observed on the surfaces; yet, when the specific myosin heavy chain is stained, it is clear that the cells are not in their physiological state. It can be concluded that neither Ti-foil nor TiO₂ NTs provide the required cues for cardiomyocytes. In addition, the quantification of cells (determined by ATP level), showed practically no viable cells on Ti-foil or TiO₂ NTs (data not shown).

The ability of both prokaryotic and eukaryotic cells to adhere, survive and grow on any surface substantially depends on the surface's chemical composition, wettability, morphology, and nanoscale morphology, and even eventually on the leaching of toxic impurities. In our study, chemical composition and wettability, as described above, did not significantly differ between the different TiO₂ NTs. Interactions with the proteins of culture media, which can influence subsequent cell adhesion and growth, should therefore be similar. Thus, it can be concluded that any differences in cell reaction can be assigned to the different surface morphologies. This is also supported by the fact that gelatinization improves the cyto-compatibility of nanostructured titanium surfaces, especially in the case of 15 nm NTs. However, the overall improvement in ESc interaction with gelatinized surfaces was not as prominent as expected, as the control surfaces and gelatinized Ti-foils seemed to provide a better environment for cell growth compared to the even gelatinized nanostructured surfaces of TiO₂.

It is also well known that different cell lines can react differently on the same surface topography, as every cell line has its specific cues, these provided by the extracellular matrix. For example, rat mesenchymal stem cells adhere, proliferate and migrate significantly better on TiO₂ NTs of 15 nm in diameter compared to flat TiO₂ [17]. With increasing diameter, cell adhesion as well as the subsequent proliferation and migration start to decline. Similarly, in the work of Bauer et al. [3], the best adhesion of MSc was detected on NTs of 15 nm in diameter, the adhesion decreasing as the NTs diameter increased further. A different situation, however, arose in a study by Lewandowska et al., in which nine different diameters of NTs (from 23 to 145 nm) were examined for

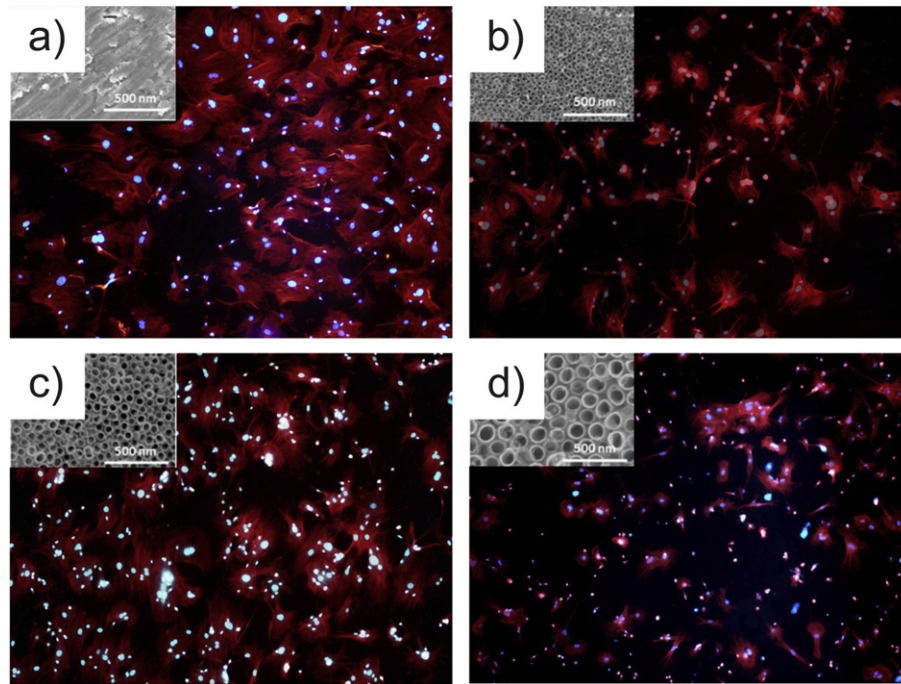


Fig. 3. Mesenchymal stem cell proliferation on a) Ti foils; b) TiO₂ NTs 15; c) TiO₂ NTs 50; d) TiO₂ NTs 100. Cell nuclei were counterstained by Hoechst 33258; the cytoskeleton was counterstained by ActinRed™ 555.

murine fibroblast adhesion and proliferation. The cell adhesion and proliferation were significantly higher for all diameters relative to pure Ti foil [11]. Remarkably, in a study by Park et al., the cell response was directly proportional to the size of NTs [17], while in a study by Lewandowska et al. this dependence was indirect. The highest level of cell proliferation was observed on the surface with a NTs diameter of 96 nm [11]. Another cell type (osteoblast) on similar diameter was used in another study [16]. It was shown that cell growth was significantly decreased after 48 h of incubation on nanostructured TiO₂ NTs with outer diameters ranging from 70 to 120 nm compared to a flat

titanium surface. Thus it is not surprising that our results are in agreement with some previous studies, while some other studies present contradictory results. For example, Xu et al. studied the adhesion and proliferation of bone marrow MS cells on titanium NTs with diameters of 30, 100 and 200 nm. While proliferation on 30 and 100 nm NTs was comparable with Ti, cell proliferation on the largest diameter was considerably reduced [21]. Likewise, Zhao et al. studied bone MS cell proliferation on NTs with diameters of 25 and 80 nm, but did not observe any statistically significant difference in the cell quantities on these two diameters after 4 days of cultivation [23]. A different situation arose in a

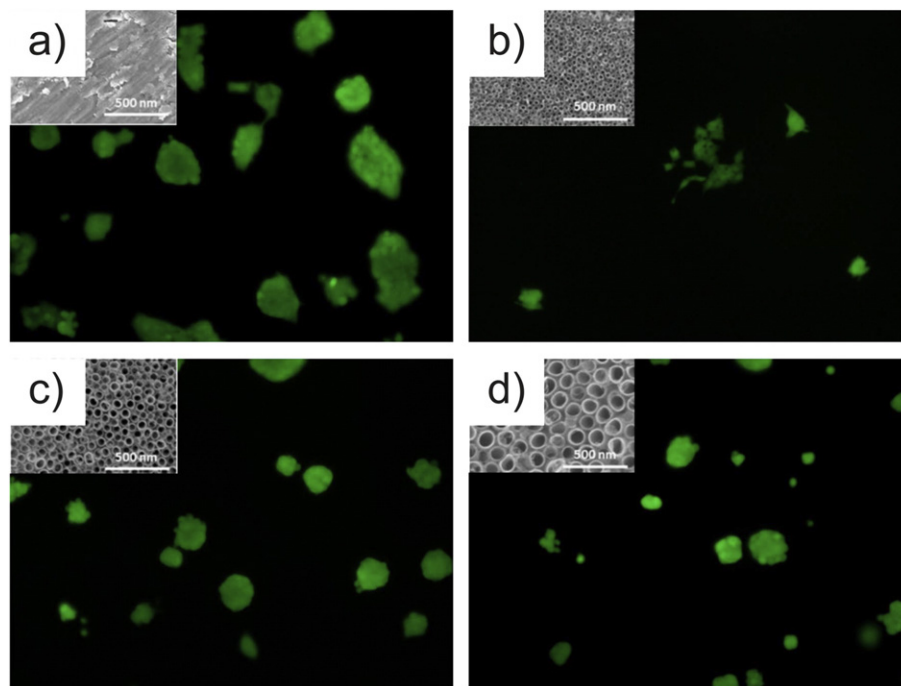


Fig. 4. Viable ESc on a) Ti foils; b) TiO₂ NTs 15; c) TiO₂ NTs 50; d) TiO₂ NTs 100 after 48 h cultivation. ESc exhibited similar morphology both on gelatinized and non-gelatinized surfaces. Only results from non-gelatinized surfaces are shown.

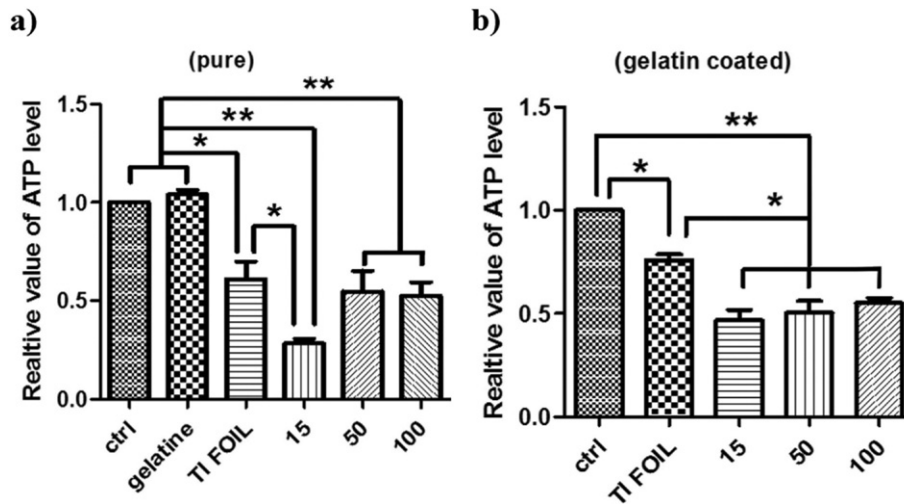


Fig. 5. Amounts of ESC cells on a) native and b) gelatine coated surfaces of individual samples after 48 h cultivation (ctrl – non-coated, TC plastic). Statistical significance was determined by ANOVA and post hoc Bonferroni's Multiple Comparison test. * marks $P < 0.05$; ** marks $P < 0.01$.

study by Park et al., in which the MS cell count decreased with the increasing diameter of NTs. Generally, the highest cell quantity was observed on 15 nm NTs and the lowest on 100 nm NTs [17].

The above-described different behaviours of MSC, ESC and cardiomyocytes show that nanostructured titanium surfaces can be used either as selective substrates for cell cultivation, or as selective surfaces for medical devices, on which only some cell lineages will be able to grow. In the case of cardiomyocytes, nanostructured surfaces could be applied for cardiac support devices, concretely in the part of devices where interactions with cardiomyocytes are not desired.

4. Conclusions

Native tissues are highly hierarchical systems with defined structures on the nanoscale level. The nanostructures of tissues, together with the biomolecules of the extracellular matrix, growth factors, and

other biologically active compounds determine cell fate. The impact of various nanostructures created on biomaterials is therefore one of the crucial parameters influencing cell behaviour and should be studied before any application is considered. In addition, the variety of cell lineages with divergent properties that specifically interact with nanotopographic features must be taken into account. In the present work, three different cell lineages – mesenchymal stem cells, embryonic stem cells, and cardiomyocytes – were seeded on nanostructured surfaces of titanium. Differences in their behaviour were studied and it was shown that mesenchymal and embryonic stem cells were able to adhere to and grow on the tested surfaces, while the contrary was observed for cardiomyocytes. Moreover, a correlation between the nanotube diameter NTs and cell behaviour was observed. The 100 nm NTs appear to present a crucial diameter for, which NTs, critically influences on mesenchymal stem cells behaviour, while the 15 nm NTs appear to present a critical diameter for embryonic stem cells. However the

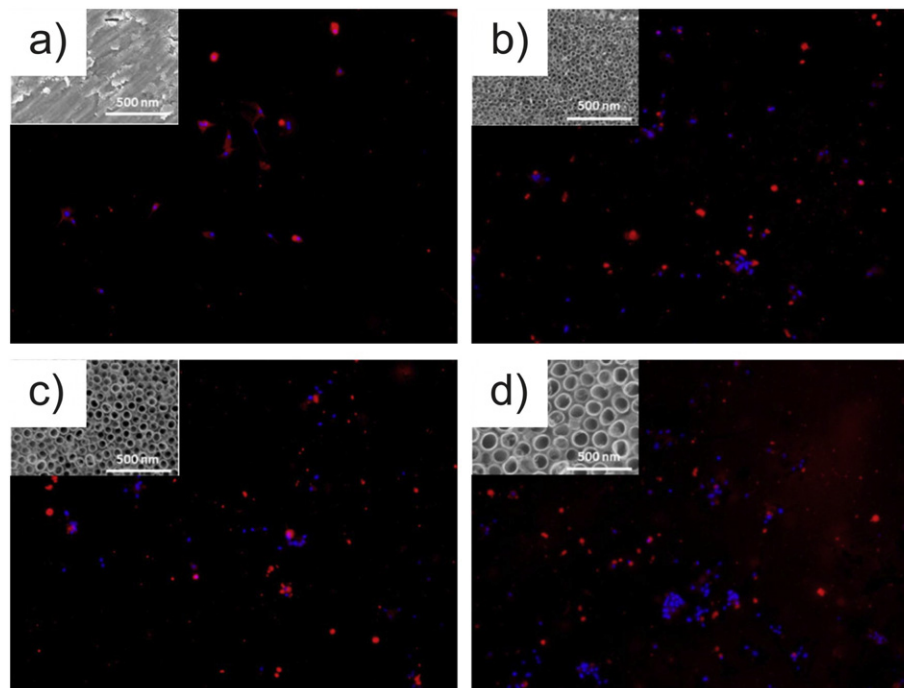


Fig. 6. HG8 cells on a) Ti foils; b) TiO_2 NTs 15; c) TiO_2 NTs 50; d) TiO_2 NTs 100 after 48 h cultivation.

behaviour of both G+ and G– biofilm-forming prokaryotic cells was similar. The results of our study provide new essential knowledge about the interaction of well-defined nanostructured titanium surfaces with two types of cell lineages, which could be of significance for the development of novel nanostructured implantable devices.

Acknowledgements

The authors are grateful to the Czech Science Foundation (17-05095S) and Slovenian Research Agency (ARRS - project L7-7566) for financial support. This work was supported by the Ministry of Education, Youth and Sports of the Czech Republic under the auspices of Program NPU I (LO1504). The authors are also grateful to Marek Koutný for help with the measurement of biofilm formation. NM is also grateful for support from an internal grant from TBU in Zlin IGA/CPS/2017/001 financed from funds for specific academic research.

References

- [1] S.P. Albu, A. Ghicov, J.M. Macak, P. Schmuki, 250 μm long anodic TiO_2 nanotubes with hexagonal self-ordering, *Phys. Status Solidi RRL* 1 (2) (2007) R65–R67.
- [2] V.C. Anitha, J. Lee, J. Lee, A.N. Banerjee, S.W. Joo, B.K. Min, Biofilm formation on a TiO_2 nanotube with controlled pore diameter and surface wettability, *Nanotechnology* 26 (6) (2015) 065102.
- [3] S. Bauer, J. Park, K. von der Mark, P. Schmuki, Improved attachment of mesenchymal stem cells on super-hydrophobic TiO_2 nanotubes, *Acta Biomater.* 4 (5) (2008) 1576–1582.
- [4] A. Flaker, M. Kulkarni, K. Mrak-Poljsak, I. Junkar, S. Cucnik, P. Zigon, A. Mazare, P. Schmuki, A. Iglic, S. Sodin-Semrl, Binding of human coronary artery endothelial cells to plasma-treated titanium dioxide nanotubes of different diameters, *J. Biomed. Mater. Res. A* 104 (5) (2016) 1113–1120.
- [5] Y. Hou, K. Cai, J. Li, X. Chen, M. Lai, Y. Hu, Z. Luo, X. Ding, D. Xu, Effects of titanium nanoparticles on adhesion, migration, proliferation, and differentiation of mesenchymal stem cells, *Int. J. Nanomedicine* 8 (2013) 3619–3630.
- [6] P. Humpolicek, K.A. Radaszkiewicz, V. Kasparkova, J. Stejskal, M. Trchova, Z. Kucekova, H. Vicarova, J. Pachernik, M. Lehocky, A. Minarik, Stem cell differentiation on conducting polyaniline, *RSC Adv.* 5 (84) (2015) 68796–68805.
- [7] M.G. Klug, M.H. Soonpaa, G.Y. Koh, L.J. Field, Genetically selected cardiomyocytes from differentiating embryonic stem cells form stable intracardiac grafts, *J. Clin. Invest.* 98 (1) (1996) 216–224.
- [8] M. Kulkarni, A. Mazare, J. Park, E. Gongadze, M.S. Killian, S. Kralj, K. von der Mark, A. Iglic, P. Schmuki, Protein interactions with layers of TiO_2 nanotube and nanopore arrays: Morphology and surface charge influence, *Acta Biomater.* 45 (2016) 357–366.
- [9] M. Kulkarni, A. Mazare, E. Gongadze, S. Perutkova, V. Kralj-Iglic, I. Milosev, P. Schmuki, A. Iglic, M. Mozetic, Titanium nanostructures for biomedical applications, *Nanotechnology* 26 (6) (2015) 062002.
- [10] M. Kulkarni, Y. Patil-Sen, I. Junkar, C.V. Kulkarni, M. Lorenzetti, A. Iglic, Wettability studies of topologically distinct titanium surfaces, *Colloids Surf. B Biointerfaces* 129 (2015) 47–53.
- [11] Z. Lewandowska, P. Piszczek, A. Radtke, T. Jedrzejewski, W. Kozak, B. Sadowska, The evaluation of the impact of titania nanotube covers morphology and crystal phase on their biological properties, *J. Mater. Sci. Mater. Med.* 26 (4) (2015) 163.
- [12] J. Macak, L. Taveira, H. Tsuchiya, K. Sirotna, J. Macak, P. Schmuki, Influence of different fluoride containing electrolytes on the formation of self-organized titania nanotubes by Ti anodization, *J. Electroceram.* 16 (1) (2006) 29–34.
- [13] H. Maleki-Ghaleh, K. Hajizadeh, A. Hajizadeh, M.S. Shakeri, S.G. Alamdari, S. Masoudfar, E. Aghaie, M. Javidi, J. Zdunek, K.J. Kurzydowski, Electrochemical and cellular behavior of ultrafine-grained titanium in vitro, *Mater. Sci. Eng., C* 39 (2014) 299–304.
- [14] A. Nagy, J. Rossant, R. Nagy, W. Abramow-Newerly, J.C. Roder, Derivation of completely cell culture-derived mice from early-passage embryonic stem cells, *Proc. Natl. Acad. Sci. U. S. A.* 90 (18) (1993) 8424–8428.
- [15] K. Narendrakumar, M. Kulkarni, O. Addison, A. Mazare, I. Junkar, P. Schmuki, R. Sammons, A. Iglic, Adherence of oral streptococci to nanostructured titanium surfaces, *Dent. Mater.* 31 (12) (2015) 1460–1468.
- [16] S. Oh, C. Daraio, L. Chen, T. Pisanic, R. Finones, S. Jin, Significantly accelerated osteoblast cell growth on aligned TiO_2 nanotubes, *J. Biomed. Mater. Res. A* 78A (1) (2006) 97–103.
- [17] J. Park, S. Bauer, K. von der Mark, P. Schmuki, Nanosize and vitality: TiO_2 nanotube diameter directs cell fate, *Nano Lett.* 7 (6) (2007) 1686–1691.
- [18] S.D. Puckett, E. Taylor, T. Raimondo, T.J. Webster, The relationship between the nanostructure of titanium surfaces and bacterial attachment, *Biomaterials* 31 (4) (2010) 706–713.
- [19] K.A. Radaszkiewicz, D. Sykorova, P. Karas, J. Kudova, L. Kohut, L. Bino, J. Vecera, J. Vitecek, L. Kubala, J. Pachernik, Simple non-invasive analysis of embryonic stem cell-derived cardiomyocytes beating in vitro, *Rev. Sci. Instrum.* 87 (2) (2016) 024301.
- [20] W. Wei, S. Berger, N. Shrestha, P. Schmuki, Ideal hexagonal order: formation of self-organized anodic oxide nanotubes and nanopores on a Ti–35Ta alloy, *J. Electrochem. Soc.* 157 (12) (2010) C409–C413.
- [21] Z. Xu, Y. Lai, D. Wu, W. Huang, S. Huang, L. Zhou, J. Chen, Increased mesenchymal stem cell response and decreased *Staphylococcus aureus* adhesion on titania nanotubes without pharmaceuticals, *Biomed. Res. Int.* (2015) 2015.
- [22] W. Yu, X. Jiang, F. Zhang, L. Xu, The effect of anatase TiO_2 nanotube layers on MC3T3-E1 preosteoblast adhesion, proliferation, and differentiation, *J. Biomed. Mater. Res. A* 94 (4) (2010) 1012–1022.
- [23] L. Zhao, L. Liu, Z. Wu, Y. Zhang, P.K. Chu, Effects of micropitted/nanotubular titania topographies on bone mesenchymal stem cell osteogenic differentiation, *Biomaterials* 33 (9) (2012) 2629–2641.